ISSN PRINT 2319 1775 Online 2320 7876
 UGC CARE Listed (Group -I) Journal Volume 11, Iss 12, 2022

The impact of using *Citrus limonum* Zinc-nano particles against leukemia cells

Huda Jameel Makki[1] and Dr. K S Chandrashekaraiah[2]

[1]Research Scholar, Department of Biochemistry, Mangalore University
[2]Research Guide, Department of Biochemistry, Mangalore University

Abstract:

In biomedical science, the environmentally friendly and economical production of metal nanoparticles is becoming increasingly significant. Zinc oxide nanoparticles (ZnO NPs) were biosynthesized in this study from Citrus limon extract, and their anticancer efficacy was evaluated utilizing several cytotoxicity assays in JURKAT cancer (Leukemia) cell lines. The morphological and structural characteristics of biogenic ZnO NPs were characterized. The synthesis was confirmed using well-known analytical techniques like UV-visible spectrophotometry, XRD, FTIR, and scanning electron microscopy. The stability of the produced NPs was also investigated. SEM and TEM were used to capture the production of cubical nanoparticles with an average size of 52nm. With a 50% inhibitory dosage of 10 g/mL, we could observe the dose-dependent rise in cytotoxicity of ZnO NPs in the JURKAT cell line.Using an MTT experiment, citrus-produced ZnNPs demonstrated lower vitality with an IC50 value of 152.54µg/ml when compared to control cells ($p<0.05$), indicating the anti-proliferating action of the nanoparticles. The amount of LDH leakage was dose-dependently increased by our eco-friendly CuNPs (IC50: 85.43±1.25µg/ml).However, it is urged that this research be expanded across various cancer models and that, in light of the results, in vivo validation be conducted.

Introduction: Cancer has emerged as the leading cause of mortality in humans, and its cost of care is also sharply rising. Lung cancer is more prevalent than other malignancies, and men and women are more likely to die from it [Mottaghitalab F, 2019]. The patients have severe side effects and induced strains due to the preceding treatment procedures, despite the availability of simple diagnosis and treatment techniques such as chemically generated medications, chemotherapy, surgery, and radiotherapy [Sreekanth T.V.M, 2018]. Researchers are now concentrating on the special qualities of nanomedicine as a substitute therapeutic method for diagnosing and treating cancer. According to the WHO's estimation, between 75 and 80 percent of the world's population still rely on traditional medicine for their medical needs [Msomi N.Z., 2018].

Cancers of the blood cells are collectively referred to as leukemia. The type of blood cell that develops into cancer and how rapidly or slowly it grows determine the type of leukemia. Although leukemia most frequently affects people over the age of 55, it is also the most prevalent disease among youngsters under the age of 15 (Swaminathan M., 2019). Leukemia has a global geographic distribution, with more industrialized nations having higher prevalence and overall mortality. However, emerging countries have a higher death rate (Tebbi CK. 2021).

The art and science of manipulating matter at the nanoscale to produce novel and distinctive materials and technologies with the great potential to transform society are known as nanotechnology. Herbicides, chemicals, or genes may be contained in nanoparticles that act as "magic bullets" and target certain plant areas to unleash their contents (Pérez-de-Luque, A., 2009). According to Nawaz, HR (2011), nano-zinc oxide offers various industrial uses, including manufacturing leather and producing rubber. Due to its high antibacterial, potential for nanonutrition, refractive index, high thermal conductivity, and UV protection properties, ZnO nanoparticle is also attracting researchers' attention for its broad application in medicine, food, agriculture, solar cells, and cosmetics (Jalal, R., 2010).

An environmentally benign method frequently used is called green synthesis or phytosynthesis of nanoparticles (Balasooriya, E.R, 2017). Due to its low cost and sparing use of hazardous chemicals, the phytosynthetic approach is an easy substitute for chemical and physical procedures. ZnO was chosen for the experiment because it has several biological uses.

Natural treatments have recently been more popularto prevent or treatvarious degenerative disorders (Paterniti I., 2014). They are frequently used to treat minor health issues but can also be combined with synthetic medications to treat more severeones. Natural medicines, vitamins, and functional foods have sparked interest among the general public, who frequently prefer using them over artificial ones. This option is recommended since it is simpler to take and has fewer side effects, which helps patients adhere to their treatment plan. As a result, natural therapies are used by up to 80% of people globally (Ferlazzo N., 2016).

A diet rich in vitamin C is recognized to lower the incidence of degenerative diseases, including cancer, and citrus limon fruits are the most often consumed in this diet (Giacosa et al., 2013). These benefits are related to various biological features, including the well-known antioxidant activity and the modulation of intracellular critical pathways involved in

degenerative processes leading to chronic diseases like cancer. Citrus fruits are one of the most significant diet sources of flavonoids. In particular, dietary flavonoids prevent carcinogen activation, promote carcinogen detoxification, scavenge free radical species, regulate cell-cycle progression, trigger apoptosis, and inhibit metastasis, angiogenesis, and cell proliferation as well as hormone or growth-factor activity (Clere et al., 2011).

Our specific goal of the study was to green synthesize ZnO NPs using *Citrus limonn*and assess its potential cytotoxic effect on JURKAT cancer cells. This was done considering the global need for solid waste management and an eco-friendly green synthesis approach.

Methods:

Preparation of plant extracts: *Citrus lemon*samples were collected from the local market and pre-washed with tap water, followed by deionized water.About 10gmof fresh samples were crushed in a pre-chilled mortar and suspended in 50ml of deionized water. The contents were boiled for 30min-45min in a water bath. After cooling, the contents were filtered and extracted with equal amounts of absolute ethanol.This precipitates the mucilage if present in the sample. The suspension was centrifuged at 5000rpm for 10min,and the supernatant collected was used for green synthesis.

Biosynthesis and characterization of Zinc oxide nanoparticles: About 30ml of ZnO (20mM) was added to 30ml of extract prepared in the previous section and suspended in 40ml of deionized water. The mixture was kept for stirring on a magnetic stirrer at 150rpm with 45^0C heating. Colour change in the mix was confirmed for nanoparticle synthesis. The reaction mixture was centrifuged at 10,000rpm for 10min, and the pellet obtained was washed with deionized water. The pellet obtained was air-dried and stored for characterization study. The reaction mixture was observed for color change depending on parameters studied, such as time, ZNO, and extract concentration at 80°C.

Stability studies: The stability of the green synthesized ZnNPs was screened at varying pHs (3, 4, 5, 6, 7, 8, 9), temperature (30-80^0C),and reaction time using UV Spectrophotometer (Shimadzu, 1800).

Characterization of silver nanoparticles: The general characteristics of nanoparticles include their size, shape, surface area, and dispersity. In many applications, these qualities' homogeneity is crucial.

UV–vis spectroscopy: On a spectrometer (Shimadzu, 1800, Japan), UV-Vis spectral experiments to obtain the surface plasmon resonance (SPR) spectra were conducted. To analyze the synthesized ZnONPs, the sample was scanned between 200 and 800 nm in wavelength at a resolution of 1nm. UV-vis Spectroscopy was used to get the absorption spectra at various pH values, temperature ranges, and metal ion concentrations. AgNPs formed as a single peak at 445nm with a cubical shape.

FTIR and XRD: The biomolecules responsible for reducing zinc salt solution into zinc nanoparticles were examined using FTIR. Following freeze-drying, the purified ZnONPs structure and composition was analyzed by scanning electron microscopy (SEM; PhilipsXL30ESEM), X-ray diffraction spectroscopy (Cu-Kα radiation (0.15406nm, Scanning speed: 5°/min; Scan range: 2θ = 20° -80°; PANalyticl, XPert Pro MPD) and Fourier transform infrared spectroscopy (400–4000cm^{-1}, 4cm^{-1}; Bomem MB100).

Dynamic light scattering (DLS): The hydrodynamic size (Z average), polydispersity index (PDI), and surface charge (zeta potential) of the greenly synthesized CuNPs were screened using the DLS method using a Horiba SZ-100 analyzer in Kyoto, Japan. Particle size was examined at a medium count rate of 210kCPS and a scattering angle of 90°.

DLS analysis: The nanoparticle tracking analysis (NTA) images showed most of the synthesized nanoparticles have an average size diameter of 60nm which was calculated based onthe Brownian motion of particles (Figure 4). The size and shape of the produced CuNps were also investigated using scanning electron microscopy. The CuNPs were primarily scattered and more or less spherical in form. The particles ranged in size from 30 to 70nm (Figure 4).

Cell culture and MTT assay: In RPMI-1640 media supplemented with 10% FBS, penicillin (100µg/ml), streptomycin (100µg/ml), and 2mM L-glutamine, human acute T-cell leukemic cell lines (JURKAT) were maintained. They were raised at 37°C in a humidified CO2 (5%)atmosphere (Król, A, 2017).

Cytotoxicity Assay: MTT ((4, 5-dimethylthiazol-2-yl)-2, 5-diphenyltetrazolium bromide) assay was conducted on JURKAT cell lines in a 96-well plate. The monolayer of cultivated cells was exposed to different doses (10, 20, 40, 80, 160, and 320µg/ml) of synthesized ZnNPs to test the cells' cytotoxicity. As a negative control, phosphate-buffered saline (PBS) was used. The cells were cultured in 100µL of RPMI media containing 25µL of MTT solution (Invitrogen Inc., USA) for 24hr. Dimethyl sulfoxide (DMSO) (Invitrogen Inc., USA)

was used to dissolve the formazan crystals generated when the MTT was converted into purple-colored formazan in living cells. An ELISA reader was used to test the solutions' absorbance at 570nm. Vinblastine (25µg/ml) was used as positive control.

LDH Assay: LDH reagent (HiMedia, India) was used to calculate the amount of LDH that leaks from cells after membrane disruption. In this experiment, the enzyme released produces a red formazan product called iodonitrotetrazolium violet, a tetrazolium salt. The quantity of lysed cells directly correlates with the amount of colour produced. As in the preceding section, cells were cultivated in various concentrations of green synthesized copper nanoparticles (10, 20, 40, 80, 160, and 320µg/ml). Vinblastine (25µg/ml) was used as positive control. After 24hr incubation, fresh media was added to all the flasks along with 50µl of LDH reagent (0.5mg/ml) and incubated for 30min at room temperature in the dark. Using an ELISA plate reader (Genetix), the absorbance was measured at 490nm after incubation. The formula used to determine the cytotoxicity caused by ZnNPs was: % cytotoxicity = Experimental LDH release / Maximum LDH release. Background media noise was eliminated. Using SPSS software, the half inhibitory concentrations (IC_{50}) of greenly synthesized ZnNPs were calculated.

Results:

Characterization study:

The UV-Vis spectra for ZnNPs are shown in Figure 1,which depictspeak absorption at 450nm. The curve depicts the formation of NPs by the reduction of Zinc salt.

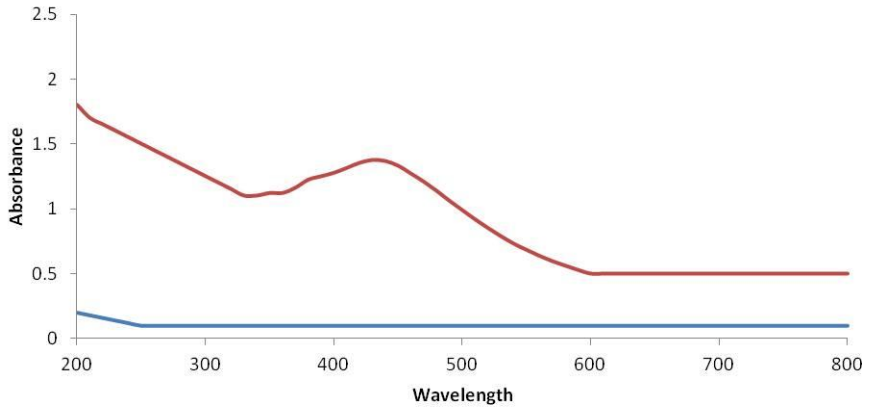

Figure 1: UV-vis spectral curve observed for the green synthesized ZnONPs from C*itrus lemon.*

ISSN PRINT 2319 1775 Online 2320 7876
 UGC CARE Listed (Group -I) Journal Volume 11, Iss 12, 2022

Stability studies:

Effect of metal salt concentration: We looked at how ZnNP formation was impacted by the concentration of zinc salt (1–40 mM) (Figure 2). According to the SPR peaks found in Figure 2, the seed formation of zinc in the synthesis of nanoparticles was found to be optimum at a concentration of 20mM. Zinc concentrations below 20mM are insufficient to create zinc seeds for the creation of nanoparticles.

Effect of reaction time: The effect of reaction time on ZnNP production was examined using UV-vis spectroscopy and the SPR peaks. Figure 3shows that peak sharpness at 436nm rises with time. Six hours of incubation time was determined to be ideal for ZnNP production.

Effect of temperature: The reaction process of silver reduction to ZnNPs is also influenced by temperature. The temperature range for the experiments was between 30 and 80°C (Figure 3). The reaction took a while to complete the reduction process, and the solution's colour changed to yellow at lower temperatures of either 30°C or 40°C. The Spectral peak at 30°C was broad, whereas the peak at 40°C was acute at 436nm. A rich brown colour of the solution was noted at or above 50°C, where metal ions transformed more quickly into nanoparticles.

Effect of pH: The effect of pH on ZnNP production was screened using UV-vis spectroscopy. Figure 2shows that peak sharpness was observed at a pH of 9. Below pH9, there was a vast peak. pH9 was determined to be ideal for ZnNP production.

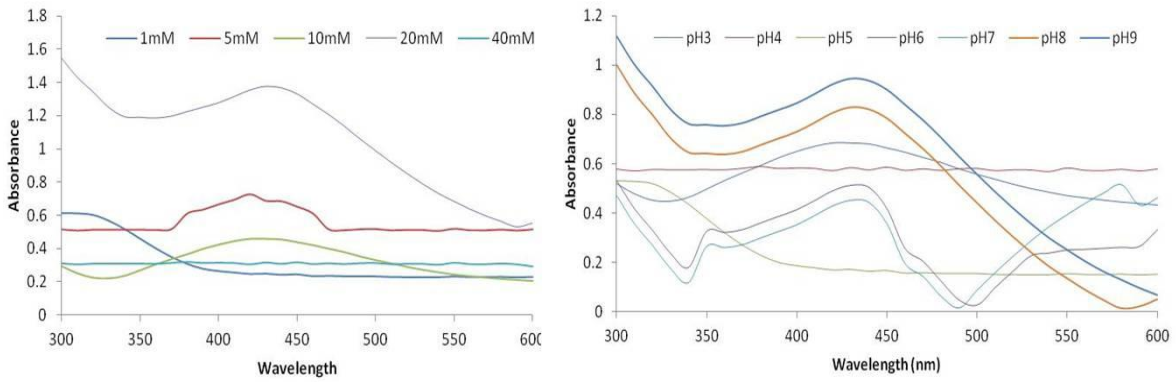

Figure 2: UV-vis spectra observed at varying metal concentrationsand pH in green synthesizing ZnONPs from C*itrus lemon.* The sample used for the synthesis is 10gm.

ISSN PRINT 2319 1775 Online 2320 7876
 UGC CARE Listed (Group -I) Journal Volume 11, Iss 12, 2022

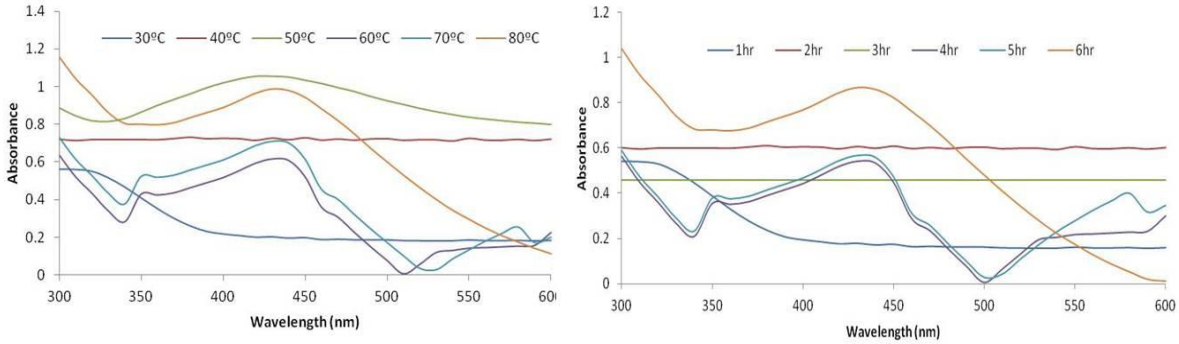

Figure 3: UV-vis spectra observed at varying temperatures and incubation time in green synthesizing ZnONPs from C*itrus lemon.* The sample used for the synthesis is 10gm.

Dynamic Light Scattering (DLS): The size distribution of the produced zinc nanoparticles was determined using the DLS under controlled conditions of ZnO (20 mM), pH 9, and temperature (500C). The average hydrodynamic size of the produced nanoparticles was around 52nm, according to the size distribution of ZnNPs (Figure 4). Zeta potential was observed at-200mV, confirming the nanoparticle synthesized's stability.

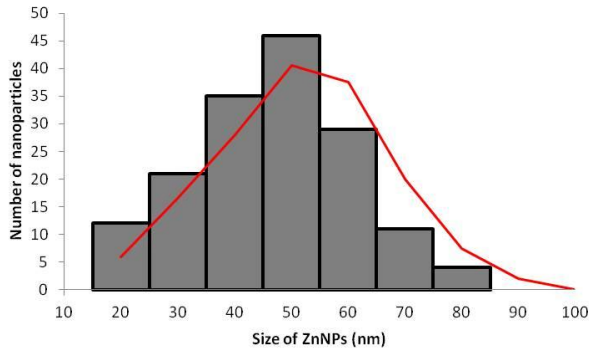

Figure 4: NTA analysis showing the distribution of ZnNPs formed at varying sizes from C*itrus lemon.*

Fourier transform infrared spectroscopy (FTIR): The FT-IR revealed the presence of a characteristic peak at about 513cm^{-1}, indicating the formation of ZnO nanostructure stretching similarly (Faye, G, 2021). FTIR of the green synthesized ZnNPs revealed the presence of 13 bands at 531, 513, 500, 486, 475, 465, 455, 450, 442, 437, 419, 412, and 405cm^{-1}. The synthesized Citrus limonum nanoparticle FTIR spectra were recorded between 500 and 4000cm^{-1} (Figure 5). This spectroscopy analyzed the different functional groups attached to nanoparticles. The peaks at 455cm^{-1} and 437cm^{-1} correspond to the O–H bond.

ISSN PRINT 2319 1775 Online 2320 7876
 UGC CARE Listed (Group -I) Journal Volume 11, Iss 12, 2022

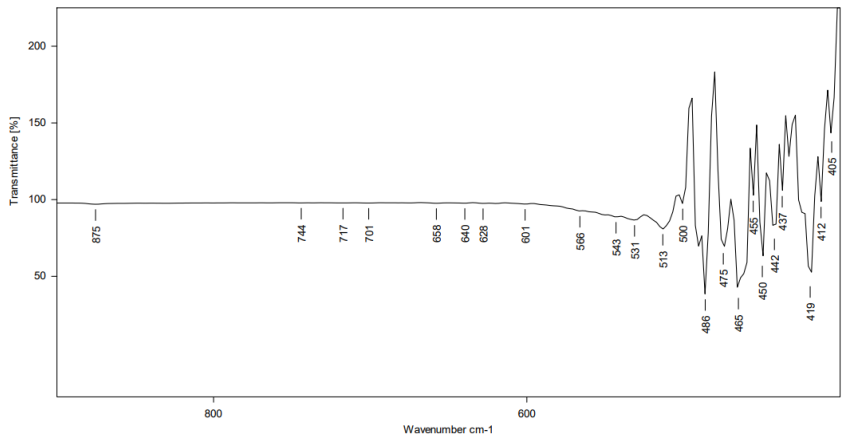

Figure 5: FTIR spectrum observed for the green synthesized ZnNPs from Lemon extract.

X-ray diffraction (XRD): The crystalline phase and orientation of the produced nanoparticles were investigated using the XRD technique. The generated Zinc nanoparticles' magnetite phase was inferred from the XRD pattern. The size of the nanoparticles was calculated from the highest peak. Additionally, the existence of organic molecules that have crystallized on the nanoparticles could be inferred from the appearance of these assigned peaks. The XRD pattern of green synthesized ZnNPs can be seen in Figure 3. The pattern clearly shows the main peaks at (2θ) = 29.3952 (135.66), 31.7617 (7443.56), 34.4218 (5069.62), 36.2460 (11935.28), 44.6126 (105.63), 47.5279(2527.97), 56.5709 (3624.67), 62.8397 (3206.64), 66.3416 (497.54), 67.9177 (2431.46), 69.0501 (1223.00), 72.5368 (223.43), 76.9195 (420.65). The brackets displayed the planes of the corresponding peaks. The shape of the ZnNPS was determined to be of the face-centered cubic geometry based on the XRD spectra shown in Figure 6.

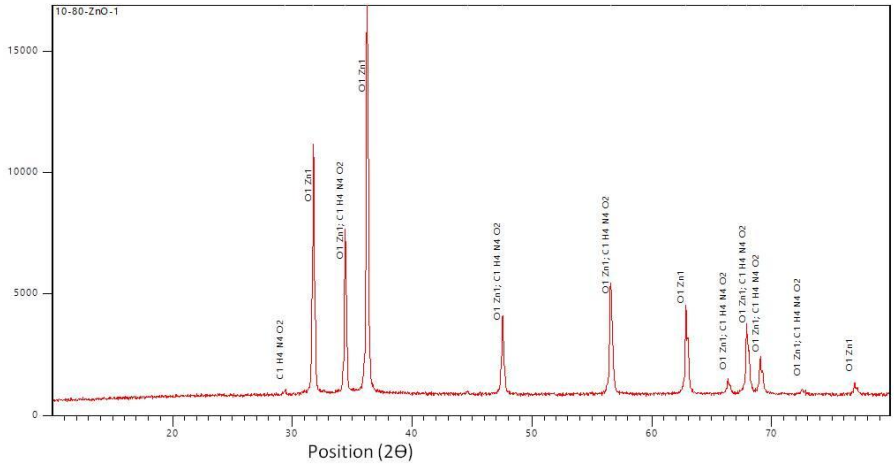

Figure 6: Spectra of X-ray powder diffraction of ZnNPs. The observed peaks usually correspond to the face-centered cubic geometry of Zinc crystals.

ISSN PRINT 2319 1775 Online 2320 7876
 UGC CARE Listed (Group -I) Journal Volume 11, Iss 12, 2022

Scanning Electron Microscopy (SEM): SEM was used to examine the surface morphology of copper nanoparticles made from synthetic *Citrus limonum*. The stabilized nanocube-like structure of the synthesized *Citrus limonum* copper nanoparticles was confirmed by SEM examination (Figure 7). The green synthesized ZnNPs were cubical and polydispersed, with a size range of 40-80nm (mean size = 52.4nm) according to SEM examination.

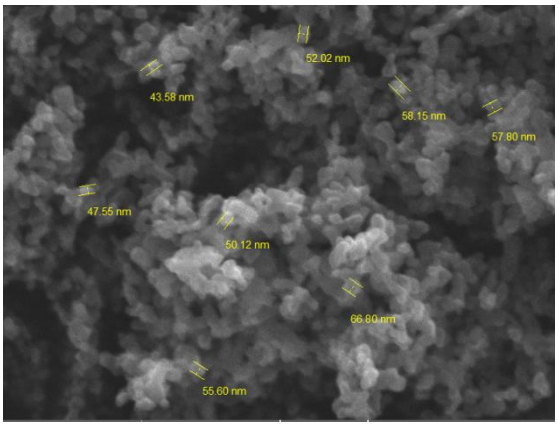

Figure 7: Photographic image of the SEM of ZnNPs synthesized from *Citrus limonum*.

Cell viability: Using the MTT reagent, a test for mitochondrial toxicity was conducted. The green synthesized ZnNPs significantly inhibited the cell viability of the cell lines used in the study at concentrations of 80µg/ml and 320µg/ml, respectively, for positive and green synthesized ZnNPs. The green synthesized ZnNPs showed inhibition of the cell lines in the range of 83 to 11 at 10 and 160µg/ml, respectively. On the other hand, positive control showed inhibition of the cell lines from 64.11 to 9.23 at 10 and 80µg/ml, respectively (Figure 8). According to Figure 8, Citrus-produced ZnNPs showed decreased vitality with an IC50 value of 152.54µg/ml compared to control cells ($p<0.05$) by MTT experiment, demonstrating the nanoparticles' anti-proliferating activity. On the other hand, positive control showed an IC50 value of 16.26µg/ml ($p<0.05$).

ISSN PRINT 2319 1775 Online 2320 7876
 UGC CARE Listed (Group -I) Journal Volume 11, Iss 12, 2022

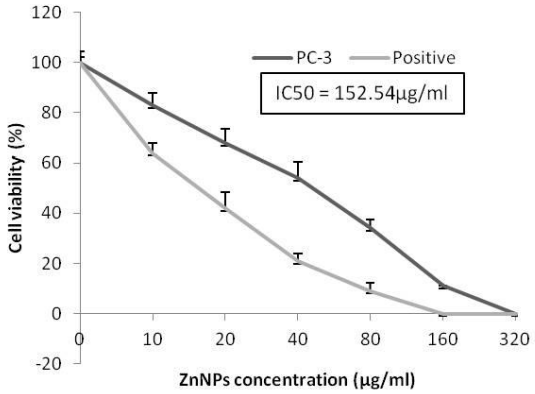

Figure 8: Graph showing the effect of ZnNPs on JURKAT cell viability. Varying concentrationsof (10, 20, 40, 80, 160, and 320µg/ml)ZnNPs were used in the study. Vincristine (50µg/ml) was used in the study. The results are represented as mean ± SD (n = 3). $p < 0.05$.

LDH assay: Our LDH assay results confirmed the results of our earlier MTT assay. Comparing the levels of cellular LDH seen in cells treated with 100% positive control to levels seen in cells treated with ZnNPs allowed researchers to assess the total cytotoxicity of the treatment. Our environmentally friendly ZnNPs showed a dose-dependent increase in LDH leakage. The cytotoxicity for the JURKAT lines was found to be from 7.12 ± 1.01 to 56.12 ± 1.32% at 10 and 320µg/ml (Figure 7). IC50 was also calculated to estimate the cytotoxic effect of green synthesized ZnNPs.AS CALCULATED, the IC50 growth inhibition values were found to be 85.43 ± 1.25µg/ml, respectively, for ZnNPs and positive control.

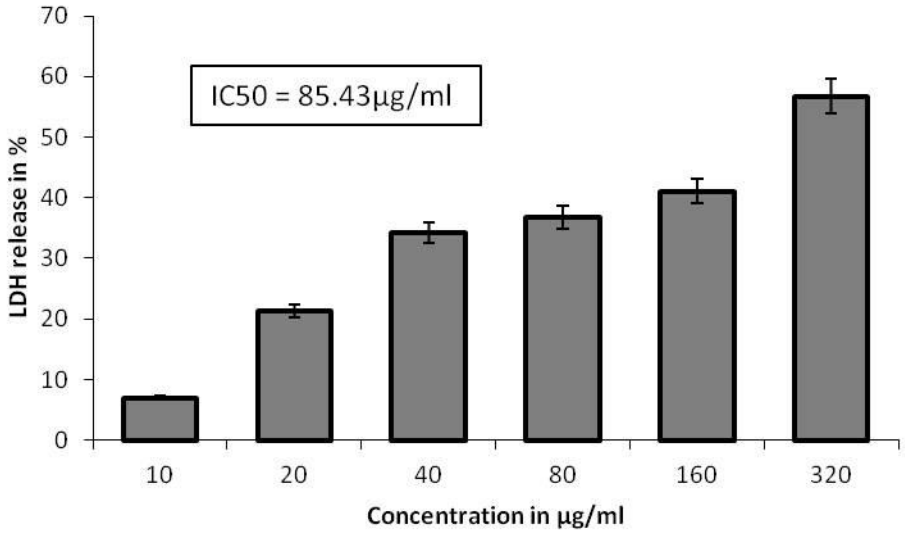

Figure: Histogram showing the percent LDH release of the green ZnNPs against the

JURKAT cell line as estimated by LDH assay. All the values are average triplicates and expressed as value ±SD ($P<0.05$).

Discussion:

This study produced ZnNPs using *Citrus limon* extract and optimized and described them. Plant extracts or green products have an advantage over the chemical or physical synthesis of NPs because of their ability to stabilize ZnNPs, intrinsic anticancerous properties, high level of efficacy, and minimum toxicity. Their use represents an NP synthesis technique that is acceptable to the environment. *According to our research, citrus limon extract has a lot of potential for the commercial synthesis of ZnNPs*.

When the greenly synthesized ZnNPs' surface plasmon resonance (SPR) properties were assessed using a UV-visible spectrophotometer, a band of absorbance at 450nm was found (Figure 2). *Raphanus sativus* and Zinc nanoparticles, which displayed a peak at 530nm, were the subject of similar reports (Umamaheswari A, 2021). Naiel, B's (2022) research revealed the UV spectra of ZnNPs at a wavelength of roughly 370nm. The ZnNPs' surface plasmon resonance primarily causes this absorption band. A similar outcome was obtained after the study of synthetic ZnNPs utilizing Sea Lavender extract [Naiel, B, 2022]. Every researcher reports a different result for NPs manufactured using various plant extracts since the surface plasmon absorbance mostly depends on the size of the NPs. The possible biomolecules in plant extract that are in charge of stabilizing and reducing ZnNP have been identified by FTIR studies. FTIR of the green synthesized ZnNPs revealed the presence of 13 bands at 531, 513, 500, 486, 475, 465, 455, 450, 442, 437, 419, 412, and 405cm^{-1}.Other studies also found corresponding peaks that were similar to this one.

Before evaluating the synthesized ZnNPs' anticancerous characteristics, it was critical to establish the particle size and charge of the materials. With the aid of the dynamic light scattering spectroscopy (DLS) method, the size and charge of the particles in an aqueous solution were identified. According to our DLS analysis (Figure 3), the average particle size of the GZnNPs was 52nm. Their charge, or Zeta potential, was also calculated to see how they might interact with other biological macromolecules, and we discovered that a charge of -200mV was generated - previous investigations into the charge and particle size of ZnNPs (Sudha, K. G., 2020).

Citrus limonn synthesized ZnNPs showed moderate to high anticancerous activity on JURKAT cell lines, as evidenced by MTT and LDH assay.The green synthesized ZnNPs showed inhibition of the cancer lines to 10% at 160µg/ml from 100% ($p<0.05$). *Citrus limonn* produced ZnNPs showed reduced viability with an IC50 value of 152.54µg/ml ($p<0.05$),as proved by the MTT experiment. Similar reports (Aldalbahi, A. *et al*., 2020; Tian W, 2020) were seen elsewhere, where several plant extract-mediated ZnNPs showed inhibition in the cell growth by MTT assay. Similar reports were seen with *C.limon* and *C.sinensis* extracts on HL-60 cell lines, where cell viability was significantly reduced. But we report the green synthesis with citrus limon for the first time. Even Camarda et al., 2007 also reported low viability in the presence of Citrus extracts on MCF-7 and K562 HL-60 cell lines.

Our study also found significant cytotoxicity on JURKAT cell lines with LDH assay. Our LDH assay results confirmed the results of our earlier MTT assay. LDH leakage was found to be 56% at 320µg/ml with an IC50 value of 85.43 ± 1.25µg/ml.Zinc oxide NPs showed similar percentage leakage in human ovarian cancer cells (Bai DP, 2017). Our results follow Kang T et al. (2013), where LDH leakage was seen in Caco-2 when treated with ZnO nanoparticles alone.

To conclude, we report the anticancerous effect of green synthesized ZnNPs from Citrus limonn for the first time. Anticancer activity was reported by ZnNPs and by Citrus limonn separately, but we studied the cooperative role of the former and the latter. We found a significant anticancer activity, as proved by MTT and LDH assay.

Conclusion: We used *Citrus limon* extracts to create ZnO NPs in an environmentally friendly manner. A change in the reaction solution's color from light yellow to dark brown with an average particle size of 52nm was the first sign that ZnO NPs were being biosynthesized. Our biogenic ZnO NPs demonstrated significant cytotoxicity in JURKAT cell lines by MTT and LDH assay, indicating their anticancer potential. The stimulation of apoptosis and enhanced ROS production seem to be the mechanism of action. To validate this unique nano-formulation, in particular in vivo model, and further exploit it for the benefit of humanity, more study in various in vitro models is required to identify the precise mechanism of action and optimum cancer model.

References:

1. Aldalbahi, A. *et al.* Greener synthesis of zinc oxide nanoparticles: Characterization and multifaceted applications. *Molecules* **25**, 25 (2020).
2. Bai DP, Zhang XF, Zhang GL, Huang YF, Gurunathan S. Zinc oxide nanoparticles induce apoptosis and autophagy in human ovarian cancer cells. Int J Nanomedicine. 2017 Sep 5;12:6521-6535. doi: 10.2147/IJN.S140071. PMID: 28919752; PMCID: PMC5592910.
3. Balasooriya, E.R., Jayasinghe, C.D., Jayawardena, U.A., Ruwanthika, R.W.D., Mendis de Silva, R. and Udagama, P.V. (2017) Honey Mediated Green Synthesis of Nanoparticles: New Era of Safe Nanotechnology. Journal of Nanomaterials, 2017, 1-10. https://doi.org/10.1155/2017/5919836
4. Camarda L., Di Stefano V., Del Bosco S. F., Schillaci D. (2007). Antiproliferative activity of *Citrus* juices and HPLC evaluation of their flavonoid composition. *Fitoterapia* 78, 426–429. 10.1016/j.fitote.2007.02.020
5. Clere N., Faure S., Martinez M. C., Andriantsitohaina R. (2011). Anticancer properties of flavonoids: roles in various stages of carcinogenesis. *Cardiovasc. Hematol. Agents Med. Chem.* 9, 62–77. 10.2174/187152511796196498
6. Faye, G., Jebessa, T. & Wubalem, T. Biosynthesis, characterization and antimicrobial activity of zinc oxide and nickel doped zinc oxide nanoparticles using *Euphorbia abyssinica* bark extract (2021).
7. Ferlazzo N., Cirmi S., Calapai G., Ventura-Spagnolo E., Gangemi S., Navarra M. (2016a). Anti-inflammatory activity of *citrus bergamia* derivatives: where do we stand? *Molecules* 21:e1273. 10.3390/molecules21101273
8. Fernandez-Bedmar Z., Anter J., de La Cruz-Ares S., Munoz-Serrano A., Alonso-Moraga A., Perez-Guisado J. (2011). Role of *citrus* juices and distinctive components in the modulation of degenerative processes: genotoxicity, antigenotoxicity, cytotoxicity, and longevity in Drosophila. *J. Toxicol. Environ. Health* 74, 1052–1066. 10.1080/15287394.2011.582306
9. Giacosa A., Barale R., Bavaresco L., Gatenby P., Gerbi V., Janssens J., et al.. (2013). Cancer prevention in Europe: the Mediterranean diet as a protective choice. *Eur. J. Cancer Prev.* 22, 90–95. 10.1097/CEJ.0b013e328354d2d7
10. Jalal, R., Goharshadi, E.K., Abareshi, M., Moosavi, M., Yousefi, A. and Nancarrow, P. (2010) ZnO Nanofluids: Green Synthesis, Characterization, and Antibacterial Activity. Materials Chemistry and Physics, 121, 198-201. https://doi.org/10.1016/j.matchemphys.2010.01.020

11. Kang, T., Guan, R., Chen, X. *et al. In vitro* toxicity of different-sized ZnO nanoparticles in Caco-2 cells. *Nanoscale Res Lett* **8**, 496 (2013). https://doi.org/10.1186/1556-276X-8-496
12. Król, A.; Pomastowski, P.; Rafińska, K.; Railean-Plugaru, V.; Buszewski, B. Zinc oxide nanoparticles: Synthesis, antiseptic activity and toxicity mechanism. *Adv. Colloid Interface Science* **2017**, *249*, 37– 52, DOI: 10.1016/j.cis.2017.07.033
13. Mottaghitalab F., Farokhi M., Fatahi Y., Atyabi F., Dinarvand R. *J. Control. Release.* 2019;295:250–267.
14. Msomi N.Z., Simelane M.B.C. InTech; Croatia: 2018. Herbal Medicine; pp. 215–227.
15. Naiel, B., Fawzy, M., Halmy, M.W.A. *et al.* Green synthesis of zinc oxide nanoparticles using Sea Lavender (*Limonium pruinosum* L. Chaz.) extract: characterization, evaluation of anti-skin cancer, antimicrobial and antioxidant potentials. *Sci Rep* **12**, 20370 (2022). https://doi.org/10.1038/s41598-022-24805-2
16. Nawaz, H.R., Solangi, B.A., Zehra, B. and Nadeem, U. (2011) Preparation of Nano Zinc Oxide and Its Application in Leather as a Retanning and Antibacterial Agent. Canadian Journal on Scientific and Industrial Research, 2, 164-170
17. Paterniti I., Cordaro M., Campolo M., Siracusa R., Cornelius C., Navarra M., et al.. (2014). Neuroprotection by association of palmitoylethanolamide with luteolin in experimental Alzheimer's disease models: the control of neuroinflammation. *CNS Neurol. Disord. Drug Targets* 13, 1530–1541. 10.2174/1871527313666140806124322
18. Pérez-de-Luque, A. and Rubiales, D. (2009) Nanotechnology for Parasitic Plant Control. Pest Management Science, 65, 540-545. https://doi.org/10.1002/ps.1732
19. Sreekanth T.V.M., Nagajyothi P.C., Muthuraman P., Enkhtaivan G., Vattikuti S.V.P., Tettey C.O., et al. *J. Photoche. Photobiol. B: Biol.* 2018;188:6–11.
20. Sudha, K. G., Ali, S., Karunakaran, G., Kowsalya, M., Kolesnikov, E., Rajeshkumar, M. P. Eco?friendly synthesis of ZnO nanorods using Cycas pschannae plant extract with excellent photocatalytic, antioxidant, and anticancer nanomedicine for lung cancer treatment. Applied Organometallic Chemistry. 2020 Apr;34(4):e5511.
21. Swaminathan M., Bannon S.A., Routbort M., Naqvi K., Kadia T.M., Takahashi K., Alvarado Y., Ravandi-Kashani F., Patel K.P., Champlin R., et al. Hematologic

ISSN PRINT 2319 1775 Online 2320 7876
 UGC CARE Listed (Group -I) Journal Volume 11, Iss 12, 2022

malignancies and Li-Fraumeni syndrome. *Cold Spring Harb. Mol. Case Stud.* 2019;5 doi: 10.1101/mcs.a003210.

22. Tebbi CK. Etiology of Acute Leukemia: A Review. Cancers (Basel). 2021 May 8;13(9):2256. doi 10.3390/cancers13092256. PMID: 34066700; PMCID: PMC8125807.
23. Tian W., Wang C., Li D., Hou H. *Future Med. Chem.* 2020;12:627–644.
24. Umamaheswari A, Prabu SL, John SA, Puratchikody A. Green synthesis of zinc oxide nanoparticles using leaf extracts of *Raphanus sativus var. Longipinnatus* and evaluation of their anticancer property in A549 cell lines. Biotechnol Rep (Amst). 2021 Feb 5;29:e00595. Doi: 10.1016/j.btre.2021.e00595. PMID: 33659193; PMCID: PMC7896141.
25. Van de Loosdrecht, A. A., Beelen, R. H. J., Ossenkoppele, G. J., Broekhoven, M. G. & Langenhuijsen, M. M. A. C. A tetrazolium-based colorimetric MTT assay to quantitate human monocyte mediated cytotoxicity against leukemic cells from cell lines and patients with acute myeloid leukemia. *J. Immunol. Methods* **174**, 25 (1994).